Molecular Determinants of the Regulation of Development and Metabolism by Neuronal eIF2# Phosphorylation in

Molecular determinants of the regulation of development and metabolism by neuronal eIF2α phosphorylation in *Caenorhabditis elegans*

Warakorn Kulalert[1], Harini Sadeeshkumar[1], Ying K. Zhang[2], Frank C. Schroeder[2] and Dennis H. Kim[1]

[1]Department of Biology, Massachusetts Institute of Technology, Cambridge, MA 02139, USA

[2]Boyce Thompson Institute and Department of Chemistry and Chemical Biology, Cornell University, Ithaca, NY 14853, USA

Correspondence: dhkim@mit.edu

Abstract

Cell-non-autonomous effects of signaling in the nervous system of animals can influence diverse aspects of organismal physiology. We previously showed that phosphorylation of Ser49 of eIF2α in two chemosensory neurons by PEK-1/PERK promotes entry of *Caenorhabditis elegans* into dauer diapause. Here, we identified and characterized the molecular determinants that confer sensitivity to effects of neuronal eIF2α phosphorylation on development and physiology of *C. elegans*. Isolation and characterization of mutations in *eif-2Ba* encoding the alpha subunit of eIF2B support a conserved role previously established by studies in yeast for eIF2Bα in providing a binding site for phosphorylated eIF2α to inhibit the exchange factor eIF2B catalytic activity that is required for translation initiation. We also identified a mutation in *eif-2c*, encoding the gamma subunit of eIF2, which confers insensitivity to the effects of phosphorylated eIF2α while also altering the requirement for eIF2Bγ. In addition, we show that constitutive expression of eIF2α carrying a phosphomimetic S49D mutation in the ASI pair of sensory neurons confers dramatic effects on growth, metabolism and reproduction in adult transgenic animals, phenocopying systemic responses to starvation. Furthermore, we show that constitutive expression of eIF2α carrying a phosphomimetic S49D mutation in the ASI neurons enhances dauer entry through bypassing the requirement for nutritionally deficient conditions. Our data suggest that the state of eIF2α phosphorylation in the ASI sensory neuron pair may modulate internal nutrient sensing and signaling pathways, with corresponding organismal effects on development and metabolism.

Phosphorylation of the alpha subunit of eukaryotic translation initiation factor 2 (eIF2α) is an evolutionarily conserved mechanism of translation control in eukaryotic cells that is pivotal for regulation of gene expression during stress (reviewed in Sonenberg and Hinnebusch, 2009). In *Saccharomyces cerevisiae*, eIF2α phosphorylation by the eIF2α kinase GCN2 promotes cellular adaptation to nutrient deficiency by attenuating global protein synthesis and preferentially upregulating translation of transcripts that are associated with stress alleviation (Hinnebusch, 2005). In mammals, four eIF2α kinases have been identified and are activated by endogenous and environmental cues that include amino acid starvation (GCN2), endoplasmic reticulum (ER) protein-folding imbalance (PERK), presence of foreign double-stranded RNA (PKR) and heme deprivation (HRI), hence constituting a homeostatic mechanism termed the Integrated Stress Response (ISR) (reviewed in Sonenberg and Hinnebusch, 2009).

Phosphorylated eIF2α attenuates protein synthesis by sequestering the guanine nucleotide exchange factor eukaryotic translation initiation factor 2B (eIF2B), the activity of which is required for the GTP-binding eIF2 to initiate translation (reviewed in Sonenberg and Hinnebusch, 2009). While the cellular consequences of eIF2α phosphorylation have been thoroughly delineated at the biochemical level (reviewed in Wek et al., 2006, reviewed in Sonenberg and Hinnebusch, 2009), recent studies have also demonstrated tissue-specific roles of phosphorylation of eIF2α in animal physiology and disease. For instance, eIF2α phosphorylation and the eIF2α kinase GCN2 have been shown to regulate intestinal homeostasis and suppress gut inflammation (Cao et al., 2014 and Ravindran et al., 2016). Recent studies have also highlighted complex physiological roles of eIF2α phosphorylation in the mammalian central nervous system.

Specifically, essential amino acid deprivation induces phosphorylation of eIF2α via GCN2 in the mammalian anterior piriform cortex to promote aversion to an amino acid-deficient diet (Hao et al., 2005 and Maurin et al., 2005). Neuronal eIF2α phosphorylation also governs synaptic plasticity and learning by modulating expression of proteins involved in both long-term potentiation and depression at hippocampal synapses (Costa-Mattioli et al., 2007 and Di Prisco et al., 2014). In addition, human genetic analyses have revealed that mutations in genes encoding translation initiation components regulating eIF2 activity such as subunits of the exchange factor eIF2B and the gamma subunit of eIF2 are associated with defects in myelination in the brain and mental disability, respectively (reviewed in Bugiani et al., 2010, Borck et al., 2012). Collectively, these findings indicate that, in addition to maintaining cellular homeostasis, neuronal eIF2α phosphorylation may exert cell-non-autonomous effects on organismal physiology and disease.

In *Caenorhabditis elegans*, environmental stressors, including those that induce translation attenuation such as nutrient limitation, trigger a state of developmental arrest termed dauer diapause, involving profound adaptations in metabolism, reproduction and behavior (Cassada and Russell, 1975). The genetic study of the dauer developmental decision of *C. elegans* has served as an experimental paradigm for understanding how environmental cues influence organismal physiology through conserved neuroendocrine signaling pathways, including insulin and transforming growth factor beta (TGFβ) (reviewed in Hu, 2007 and Fielenbach and Antebi, 2008). In a previous study, we characterized the mechanism by which the *daf-28(sa191)* mutation, previously isolated and molecularly characterized as a mutation in a gene encoding an insulin ligand (Malone and Thomas, 1994 and Li et al., 2003), causes constitutive dauer entry.

The R37C substitution in the DAF-28 insulin peptide causes endoplasmic reticulum stress specifically in the ASI chemosensory neurons, activating the Unfolded Protein Response regulator PEK-1/PERK, which phosphorylates a conserved regulatory Ser49 in eIF2α in the ASI chemosensory neuron pair to promote entry into dauer diapause (Kulalert and Kim, 2013). Because DAF-28 itself has been previously established to function redundantly to inhibit dauer formation (Cornils et al., 2011 and Hung et al., 2014), UPR activation and PEK-1-mediated eIF2α phosphorylation act in conjunction with the lack of functional anti-dauer DAF-28 in the *daf-28(sa191)* mutant to confer a strong constitutive dauer entry phenotype in this mutant background.

Here, to further characterize the mechanism underlying the organismal response to this neuron-specific eIF2α phosphorylation, we sought to isolate mutations that could suppress the constitutive dauer entry phenotype of the *daf-28(sa191)* mutant. We have identified conserved mechanisms mediating sensitivity to eIF2α phosphorylation in the nervous system of *C. elegans*. We also characterize developmental and metabolic phenotypes of animals expressing an *eIF2α* transgene carrying a phosphomimetic S49D mutation, which suggest a cell-non-autonomous role for the state of eIF2α phosphorylation in the ASI sensory neuron pair in modulating the organismal response to nutrient deficiency.

Materials and Methods

Caenorhabditis elegans strains

C. elegans strains were maintained as previously described (Brenner, 1974). Strains used in this study are listed in Table S3.

Suppressor mutant isolation and characterization

Mutagenesis using ethyl methanesulfonate (EMS) was performed on the starting strain carrying the *daf-28(sa191)* allele. F2 generation eggs from sixteen independent F1 generation pools were plated onto NGM plates seeded with *E. coli* strain OP50. The plates were screened for F2 animals that, unlike the starting strain, failed to enter dauer diapause 48 hours later at 25ºC. Specifically, we isolated L4 or young adult F2 animals. The recovered mutants were retested and selected based on viability and the ability to give rise to largely non-dauer population in subsequent generations.

We then crossed the mutants into the starting strain to determine mode of inheritance. For recessive suppressor mutants, complementation testing was performed using the previously characterized suppressor *daf-28(sa191);pek-1(ok275)* strain (Kulalert and Kim, 2013) and the *eif-2Ba(qd335);daf-28(sa191)* mutant (see recessive *eif-2Ba* alleles in Table S2). Representative dominant mutants were outcrossed at least three times to the starting strain and were submitted for whole genome resequencing and bioinformatics analyses, performed by BGI Americas. We then identified nucleotide polymorphisms that were unique to each mutant, and used existing deletion or presumptive null alleles (*daf-28(tm2308)*, *erp-44.1(gk411949)* and *eif-2Ba(pk720)*) to determine whether loss-of-function mutations in the genes contribute to the phenotypic suppression. Sanger sequencing was used to identify additional alleles of the candidate genes in

the remaining mutants. For *eif-2Ba*, we also performed cell-specific rescue to confirm that EIF-2Ba functions in the ASI neurons to promote dauer formation in response to neuronal eIF2α phosphorylation (Figure 1B).

Constructs and generation of transgenic animals

The promoter of the *gpa-4* gene was used as an ASI-specific promoter to express transgenes (Jansen et al., 1999, Bishop and Guarente, 2007). Importantly, the *gpa-4* promoter was able to drive heterologous gene expression to mediate organismal phenotypes in both larval and adult stages, specifically dauer formation and diet-restriction-mediated lifespan extension (Bishop and Guarente, 2007, Kulalert and Kim, 2013).

We also utilized *str-3p* to drive neuron-specific expression of *eif-2Ba* in Figure 1B. Plasmids containing *str-3p::eif-2Ba::unc-54 3′UTR* (70 ng/μL) and *ofm-1p::GFP* (80 ng/μL) were used to generate transgenic animals, and three independent lines were recovered and propagated.

As described in Evans, 2006, gamma radiation was employed to integrate the *qdIs10[gpa-4p::eIF2α(S49D)]* extrachromosomal arrays. The animals carrying the integrated arrays were then outcrossed nine times. Animals carrying extrachromosomal (Kulalert and Kim, 2013 and Figure S5) or integrated arrays both exhibited similar starvation-like phenotypes.

Dauer formation assay

Six to eight gravid animals were picked to individual well-seeded 6-cm NGM plates, allowed to lay eggs at the assay temperature for three to six hours, and removed. Live *E. coli* strain OP50

was used as a food source. For the assays conducted at 25ºC, dauer and L4 larvae were scored at 48 hours after the egg-lay midpoint, as at this time point all the animals have passed the pre-dauer stages and, for the dauer-constitutive mutants that exit dauer, the dauer larvae have not resumed reproductive development. Dauers were discriminated from non-dauers based on radial shrinkage of the body, the absence of pharyngeal pumping, and an overall dark appearance (Cassada and Russell, 1975). To minimize variation in environmental conditions that could influence dauer formation, the same position in the incubator was used in all the experiments for temperature consistency, and the population density on each plate was controlled by the number of gravid adults laying eggs and the duration of egg-lay.

Unless otherwise noted, all dauer formation assays were done without ascarosides. In Figures 5B and 5C, 100 μL of the pheromone mix consisting of synthetic ascarosides #2, #3, #5 and #8 (Pungaliya et al., 2009) was added onto 3.5 cm plates made with Noble agar and without peptone. Concentrated heat-killed or live *E. coli* OP50 were then seeded onto the plates. Egg laying was done at 25°C using around three adults of indicated genotypes for 3-5 hours, and scoring took place 72 hours afterward. The average total number of animals per plate was approximately 40 to 60.

Brood size assay

Individual L4 animals were placed onto NGM plates seeded with *E. coli* strain OP50 at 25ºC. Each animal was then transferred to individual plates on a daily basis for at least five days. The number of eggs laid or progeny hatched was then scored every day. The results shown were based on multiple animals from at least two independent experiments.

RNAi-dependent assays

RNAi by bacterial feeding using *E. coli* HT115 bacteria was carried out as reported. All vectors used in this study were validated by Sanger sequencing. For each experiment, bacteria expressing the empty L4440 vector (negative control RNAi), the L4440-derived *unc-22* RNAi vector (positive control RNAi, based on the twitching phenotype induced by *unc-22* knockdown) and the respective L4440-derived translation regulatory factor gene RNAi vectors were included. L4 animals were fed on RNAi bacteria plates for 72 hours at 16ºC, and the F_1 generation animals were scored for fractions that reached L4 and subsequent fertile adulthood at 25ºC. Results shown were based on multiple independent experiments.

Microscopy

Animals at indicated developmental stages were mounted with 10mM sodium azide onto slides with a 2% agarose pad. The slides were viewed using an AxioImager Z1 fluorescence microscope (Zeiss) with indicated objectives. The fluorescence signals were recorded by a CCD camera (AxioCam), using constant exposure time without saturation for each experiment.

For lipid storage visualization, Sudan Black staining was performed, using a protocol adapted from Kimura et al., 1997. Specifically, animals were fixed in 1% formaldehyde, stained with 50% Sudan Black solution and washed in M9 buffer four times before mounting.

Data availability

Strains are available upon request.

Results and Discussion

Isolation and characterization of mutations that suppress the dauer-constitutive phenotype of *daf-28(sa191)*

We mutagenized approximately 40,000 genomes of *daf-28(sa191)* animals and isolated mutants that exhibited suppression of the dauer-constitutive phenotype of the starting strain (Figure S1). We then employed complementation testing and whole genome sequencing to identify candidate genes. Our prior study suggested that expression of the mutant R37C DAF-28 insulin peptide in the ASI neurons causes endoplasmic reticulum stress, activating the Unfolded Protein Response and leading to activation of PERK/PEK-1, which phosphorylates eIF2α (Kulalert and Kim, 2013). Consistent with our model, we isolated mutations affecting each of these steps (Figure 1A).

Mutations likely affecting the phosphorylation of eIF2α induced by the expression of toxic mutant R37C DAF-28:

First, we isolated second-site, revertant mutations in the gene encoding the mutant DAF-28 insulin (Figure 1A and Table 1). We identified a presumptive null allele of *daf-28,* which carries an additional missense mutation in the start codon (M1X R37C), preventing translation initiation of the toxic peptide. The absence of the toxic mutant DAF-28 likely abrogates ER protein folding imbalance that triggers neuronal eIF2α phosphorylation and dauer formation through PEK-1. Consistent with this hypothesis, we note that the analysis of trans-heterozygote animals carrying two distinct alleles of *daf-28* suggest that this allele of *daf-28* behaves similarly to the null *daf-28(tm2308)* deletion allele (Figure S2). We also isolated another allele of *daf-28,* which results in

a premature truncation of the peptide (R37C Q81X). Trans-heterozygote analysis suggests that this allele acts similarly to the wild-type *daf-28* allele (Figure S2), leading us to speculate that the 16-amino-acid truncation, while having no effect on DAF-28 function, may restore pairings of cysteine residues, circumventing the ER-toxic consequences of exposed reactive thiol moieties of unpaired cysteines that promote dauer formation. The recovery of the loss-of-function and revertant alleles of *daf-28* further underscores insulin misprocessing as a source of ER homeostasis perturbation, and suggests proteotoxic contributions of unpaired cysteine, as in the case of the Akita diabetes mouse model (Figure S2 and Wang et al, 1999).

Second, we isolated three presumptive null alleles of a previously uncharacterized gene *c30h7.2* (Figure 1A and Table 1). The suppression of the dauer entry phenotype was also confirmed by a previously generated null allele of *c30h7.2*, *gk411949* (fraction of *c30h7.2(gk411949);daf-28(sa191)* dauers = 0.02 ± 0.02; N = 228). The gene encodes an ortholog of mammalian ERp44, which is a member of the protein-disulfide isomerase family (Anelli et al., 2002 and Anelli et al., 2003). ERp44 is involved in quality control of several ER client proteins (Higo et al., 2005, Freyaldenhoven et al., 2012, Hisatsune et al., 2015, Yang et al., 2016). Importantly, ERp44 has been shown to directly interact with proinsulin in mouse insulinoma cells (Pottekat et al., 2013). Because loss-of-function mutations of *c30h7.2* suppressed the organismal consequences of ER toxicity, we hypothesized that ERp44 may participate in formation or retention of the toxic DAF-28(R37C)-derived complexes that activate the Unfolded Protein Response (UPR) to promote dauer entry. Consistent with this hypothesis, we observed reduction of neuronal UPR activation in the absence of ERp44, suggesting that the isomerase contributes to the ER toxicity triggered by the mutant neuronal insulin (Figure S3). Our genetic analysis of the *C. elegans* ERp44 points

to a conserved function of the disulfide isomerase in modulating maturation of insulin (Figure S3 and Pottekat et al., 2013).

Third, as anticipated by our prior study (Kulalert and Kim, 2013), we isolated eighteen alleles of *pek-1,* which encodes the *C. elegans* ortholog of mammalian eIF2α kinase PERK that is activated by the toxic-peptide-mediated disruption of protein folding homeostasis in the ER (Figure 1A and Table 1). In addition to nonsense substitutions that lead to premature truncation of PEK-1, the remaining of the recovered *pek-1* alleles harbor alterations in the residues in the conserved cytoplasmic kinase and ER luminal domains of PEK-1 (Figure S1 and Table S1).

Fourth, we recovered an allele of eIF2α (*eif-2a/y37e3.10*) that results in an S49F substitution at the conserved Ser49 target of eIF2α kinases (Figure 1A and Table 1). Suppression of the dauer entry phenotype by this *eIF2α* allele further corroborates our genetic analysis of phosphomimetic (S49D) and unphosphorylatable (S49A) transgenes expressed in the ASI neuron pair, which implicated a pivotal role for eIF2α in promoting entry into dauer diapause (Kulalert and Kim, 2013).

Mutations in eIF2Bα/EIF-2Ba altering sensitivity to eIF2α phosphorylation:

Translation initiation requires guanine nucleotide exchange on eIF2 mediated by the multimeric eIF2B (reviewed in Sonenberg and Hinnebusch, 2009). Molecular genetic studies in yeast have established that eIF2Bα is a non-essential, regulatory subunit that provides a binding site for phosphorylated eIF2α (eIF2(αP)) to inhibit the eIF2B Guanine Exchange Factor (GEF) activity required for translation initiation (Yang and Hinnebusch, 1996).

We isolated eleven distinct suppressor mutations in the gene encoding the *C. elegans* ortholog of the alpha subunit of eIF2B (*eif-2Ba*), *zk1098.4* (Table 1). Two presumptive null alleles of *eif-2Ba* also suppressed the constitutive dauer entry phenotype (see *qd335* in Table 1; for the *eif-2Ba(pk720)* deletion allele, fraction of *eif-2Ba(pk720);daf-28(sa191)* dauers = 0.02 ± 0.02; N = 133), consistent with the dispensable, regulatory role of GCN3/eIF2Bα in *S. cerevisiae* (Yang and Hinnebusch, 1996). Overexpression of *eif-2Ba* specifically in the ASI neurons was able to restore the constitutive dauer entry phenotype of the *eif-2Ba(qd335);daf-28(sa191)* mutant, indicating that EIF-2Ba functions in the two neurons to promote the dauer developmental decision in response to neuronal eIF2α phosphorylation (Figure 1B). Most of the *eif-2Ba* alleles isolated conferred the suppression in a dominant fashion, similar to the *eif-2Ba* deletion allele (Table S2). The dominant nature of the *eif-2Ba* deletion allele in suppressing the organismal response to eIF2α phosphorylation suggests that eIF2B susceptibility to eIF2(αP) is readily perturbed by reduced eIF2Bα dosage. The *eif-2Ba* mutations that confer the dominant suppressor phenotype similar to the loss-of-function allele likely affect residues that are critical for eIF2Bα functional and structural integrity (Table S2). Additionally, because eIF2Bα forms a homodimer as part of the eIF2B holoenzyme, the altered eIF2Bα may exert a dominant-negative effect that prevents proper dimerization or holoenzyme formation (Kashiwagi et al., 2016).

We note that four *eif-2Ba* mutations alter residues that are conserved not only among eIF2Bα across species but also among the equivalent domains in the other regulatory subunits of eIF2B that recognize eIF2(αP), β and δ, suggesting pivotal regulatory functions (Table S2). A number of previously characterized eIF2(αP)-insensitive mutations in yeast eIF2B subunits α, β and δ

also affect residues and domains shared among all three regulatory subunits (Pavitt et al., 1997). Of note, a number of *S. cerevisiae* hypomorphic alleles of *GCD7/eIF2Bβ* and *GCD2/eIF2Bδ* that render the yeast cells refractory to the inhibitory effects of eIF2α phosphorylation have been characterized (Vazquez de Aldana and Hinnebusch, 1994). While we isolated eleven loss-of-function alleles of *eif-2Ba*, no alleles of the genes encoding the other two regulatory subunits, β and δ, were recovered. We observed that the beta and delta subunits of eIF2B, unlike the alpha subunit, are essential for *C. elegans* development (Figure 2C). Our data suggest a conserved molecular target and mechanism in response to eIF2α phosphorylation in *C. elegans* (Figure 1A).

Remarkably, over 120 mutations in genes encoding human eIF2B subunits have been associated with Vanishing White Matter Disease, which involves hypomyelination in the central nervous system (reviewed in Bugiani et al., 2010). The enrichment of neuropathology-associated eIF2B mutant alleles suggests critical roles of eIF2B subunits in regulating homeostasis and myelin formation function of glial cells in the mammalian brain (Lin et al., 2014). We also note that eIF2B regulatory subunit δ has been identified as the molecular target of the drug ISRIB that renders mammalian neurons refractory to eIF2α phosphorylation to enhance memory formation (Sidrauski et al., 2015 and Sekine at al., 2015). These findings illustrate critical roles of eIF2B-mediated translational control in the nervous system of higher animals, in addition to the worm model.

Isolation and characterization of an unusual mutation in eIF2γ/EIF-2c:

The translation factor eIF2 is a G-protein complex composed of three distinct subunits, alpha, beta and gamma (reviewed in Sonenberg and Hinnebusch, 2009). We identified a mutation in the *C. elegans* ortholog of the guanine nucleotide-binding gamma subunit of eIF2 (*eif-2c*), *y39g10ar.8* (Figure 1A and Table 1), which conferred dauer suppression in a dominant manner, suggesting alteration of function of this essential factor. The *qd336* mutation alters a conserved serine residue in domain III of eIF2γ (Roll-Mecak et al, 2003), resulting in an S443L substitution.

The isolation of an unusual allele of *eif-2c(qd336)* that can confer insensitivity to the effects of eIF2(αP) was reminiscent of a previously characterized mutation in *GCD11(K250R),* the yeast ortholog of *eIF2γ*, which obviates the need for the GEF eIF2B in protein synthesis (Erickson and Hannig, 1996 and Erickson et al., 2001). Such diminished reliance on eIF2B would relieve translation initiation from regulation by eIF2(αP)-mediated eIF2B sequestration. We examined if the *eif-2c(qd336)* mutation could also enable eIF2B-independent translation initiation by performing RNAi knockdown of individual eIF2B subunits to assess whether the *eIF2γ* mutant can bypass the requirement for eIF2B during larval development. RNAi knockdown of expression of the essential subunits eIF2Bβ, eIF2Bδ, eIF2Bγ and eIF2Bε inhibited larval development in the wild-type background (Figure 2B). Strikingly, we observed that the *eif-2c(qd336)* mutant developed normally and reached reproductive maturation in the absence of eIF2Bγ, while still failing to survive when expression of the other essential eIF2B subunits had been impaired by RNAi (Figures 2A and 2B).

We note that the ability to circumvent the requirement for eIF2Bγ is unique to the *eif-2c(qd336)* mutant, and does not occur in the other eIF2(αP)-resistant mutants isolated from the screen (Figure 2D). The S443L substitution in eIF2γ also confers insensitivity to eIF2α phosphorylation via a distinct mechanism from the aforementioned *S. cerevisiae GCD11(K250R)* mutation (Erickson and Hannig, 1996 and Erickson et al., 2001), as the *C. elegans eIF2γ(S443L)* mutation did not result in growth impairment or bypass of the essential functions of eIF2α and all essential eIF2B subunits (Figures 2B and 2C, compared to Erickson et al., 2001). Indeed, the *eif-2c(qd336)* mutant still requires the key catalytic subunit eIF2Bε that mediates the nucleotide exchange activity (Figure 2B). Because EIF-2c(S443L) can functionally substitute for the eIF2Bγ subunit, but not for eIF2Bε (Figure 2B), the alternative mechanism underlying eIF2(αP) resistance is likely to involve a molecular event catalyzed exclusively or predominantly by eIF2Bγ, which is not the GTP-GDP exchange that is largely mediated by eIF2Bε (Pavitt et al., 1998). The eIF2Bγ subunit has been shown to also participate in the displacement of the translational regulatory factor eIF5 that prevents GDP dissociation from the translation-incompetent eIF2-GDP complex, thus antagonizing the exchange activity of eIF2B required for translation initiation (Jennings et al., 2013). It is plausible that the S443L change in eIF2γ facilitates the displacement of eIF5, bypassing the requirement for eIF2Bγ in dissociating eIF5 from eIF2 to promote translation-competent eIF2 complex formation. The augmented dissociation of eIF5 contributed by the mutant eIF2γ(S443L) may diminish the requirement for this specific eIF2B function in eIF5 displacement, altering sensitivity to reduced eIF2B activity when eIF2α is phosphorylated. Furthermore, in addition to sequestering eIF2B, phosphorylation of eIF2α has been postulated to enhance the abundance of the translation-incompetent eIF2-eIF5 complex (Jennings and Pavitt, 2010). Therefore, the eIF2γ(S443L) alteration that destabilizes

and depletes the eIF2(αP)-induced translation-incompetent eIF2-eIF5 complexes would also undermine such translation inhibitory consequences of eIF2α phosphorylation.

We have demonstrated that the eIF2Bγ-specific functional or structural roles are dispensable in the *eif-2c(qd336)* mutant background (Figure 2B), likely resulting in reduced dependence on eIF2B and thus diminishing the inhibitory effects of eIF2(αP) on eIF2B functions and translation initiation (Figure 2A). We note that our mechanistic interpretations and distinctions among different eIF2 subunit mutants are mainly derived from the extensive genetic and biochemical studies conducted in yeast, in light of the high evolutionary conservation of residues and domains across eukaryotes. Importantly, our genetic characterization of the mechanistically distinct *eif-2c(qd336)* mutant unambiguously demonstrates that a subset of eIF2B catalytic functions is dispensable for translation initiation and organismal viability, enabling eIF2B-compensatory mechanisms to bypass translational regulation by eIF2α phosphorylation that targets eIF2B.

Physiological consequences of phosphomimetic eIF2α(S49D) expression in the ASI neurons

Having defined mutants unable to respond to the effects of eIF2α phosphorylation, we sought to next examine the effects of increased eIF2α phosphorylation. Based on the insights gained from the study of the *daf-28(sa191)* mutant in which eIF2α phosphorylation is induced in the ASI neuron pair, we sought to further investigate the effects of increased eIF2α phosphorylation specifically in the ASI neuron pair. We examined animals carrying an integrated transgene expressing phosphomimetic *C. elegans* eIF2α(S49D) in the ASI neuron pair, which resulted in

readily observed effects on growth, reproduction, metabolism, and the dauer developmental decision.

Expression of phosphomimetic eIF2α(S49D) in the ASI neuron pair mimics organismal phenotypes associated with nutrient deficiency:

In adult hermaphrodite animals, expression of phosphomimetic eIF2α in the ASI neuron pair resulted in small body size (Figures 3A, 3B and 3C), consistent with diminished growth rate (Figure 3D). The animals expressing eIF2α(S49D) in the ASI neurons also exhibited clear appearances, consistent with diminished fat storage observed (Figure 3H). We also noted a significantly reduced brood size and an extension of the egg-laying period in the animals carrying the neuron-specific phosphomimetic eIF2α transgene, in comparison to the wild-type control (Figures 3E and 3G). Unlike wild-type animals that stored 10-15 fertilized eggs *in utero*, the animals with ectopic neuronal eIF2α phosphorylation harbored a drastically reduced number of fertilized embryos (Figure 3F). The impairment in development and progeny production was independent of rearing temperature. Notably, these reproductive and metabolic defects are reminiscent of those occurring in animals that were defective in feeding or subjected to unfavorable conditions that promote reallocation of resources and germ cell death, such as starvation (Avery, 1993 and Angelo and Van Gilst, 2009). Further corroborating the cell-non-autonomous influence of neuronal eIF2α phosphorylation on gene expression and metabolism, we observed downregulation of *atgl-1*, which encodes a lipase that functions in the intestine (Figure 3I). Such alteration in gene expression in distal tissues may suggest an adaptive role of the organismal consequences of neuron-specific eIF2(αP), for instance in preventing exhaustion of the energy reserve.

Expression of wild-type and unphosphorylatable versions of eIF2α in the ASI neuron pair did not result in diminished progeny production or extended egg-laying period, indicating that the reproductive impairment is phosphorylation-status-specific. (Figure S5). In addition, the systemic defects driven by the neuronal phosphomimetic eIF2α were significantly suppressed by the *eif-2Ba* and *eif-2c* mutations that confer insensitivity to eIF2α phosphorylation (Figures 4A and 4B). The suppression of diverse physiological effects of ectopic neuronal eIF2(αP) by *eif-2Ba* and *eif-2c* mutations (Figures 1, 4A, 4B and 5C) underscores the roles of the *C. elegans* eIF2Bα and eIF2γ in mediating organismal sensitivity to phosphorylation of eIF2α throughout life. Moreover, we observed that genetic ablation of the ASI neurons, unlike constitutive eIF2α phosphorylation, had no effect on non-dauer growth and reproduction (Figures 4C and 4D), suggesting that general neuronal dysfunction or death did not account for the systemic phenotypes in response to the phosphorylation state of eIF2α.

Expression of phosphomimetic eIF2α in the ASI neuron pair acts with pheromone to promote dauer entry even under optimal bacterial food conditions:

We also observed that the animals carrying the *qdIs10* transgene expressing phosphomimetic eIF2α in the ASI neuron pair, while not exhibiting the constitutive entry phenotype at the standard assay population density, were more prone to entering dauers when the plates became crowded without food deprivation. Additionally, constitutive neuronal eIF2α phosphorylation was sufficient to enhance dauer formation in the insulin- and TGFβ-deficient genetic backgrounds, which partially sensitize the animals to form dauer larvae (Figure 5A). Overexpression of wild-type eIF2α, unlike the phosphomimetic variant, has been shown to have

no effect on the dauer decision (Kulalert and Kim, 2013), indicating that the developmental effect elicited by the *qdIs10* transgene is phosphorylation-status-specific. Taken together, these observations suggest that, during larval development, ASI-specific eIF2α phosphorylation synergizes with other previously characterized dauer-promoting inputs including crowding and aberrant neuroendocrine signaling levels to trigger entry into diapause.

A robust method to induce dauer formation of wild type animals in the laboratory is treatment with assortments of ascarosides in the presence of heat-killed *E. coli*, as live bacteria confer inhibitory effects on dauer formation (Figure 5B, Jeong et al., 2005, Kim et al., 2009, McGrath et al., 2011 and Park et al., 2012). The molecular basis of the requirement for heat-killed bacteria to efficiently induce dauer entry in the presence of dauer pheromone in the laboratory remains unclear. Non-dauer animals grown on heat-killed *E. coli* exhibit impaired growth and reproduction, indicative of exposure to a poor nutritional source. It is thus plausible that the nutritionally deficient nature of heat-killed bacteria contributes to robust dauer formation observed in the pheromone assay. Because constitutive eIF2α phosphorylation in the ASI neurons, which integrate both dauer pheromone and food signals, phenocopies responses to food scarcity in adult animals (Figure 3), we hypothesize that ASI-specific phosphorylation of eIF2α may also confer similar anti-growth effects during larval development, mimicking nutritionally deficient conditions that enhance dauer formation in the presence of dauer pheromone.

Corroborating our hypothesis, the animals carrying the ASI-specific phosphomimetic *eIF2α(S49D)* transgene formed dauers efficiently even in the presence of dauer pheromone and live bacteria, the pro-growth food source that largely suppressed dauer entry in wild-type control

(Figure 5C). Importantly, constitutive phosphorylation of eIF2α in ASI is not sufficient to promote dauer formation without the presence of dauer pheromone, indicating that aberrant neuronal eIF2α phosphorylation status may only specifically modulate food-dependent sensitivity to the ascarosides. The ability of the *qdIs10* transgene to promote dauer formation in response to dauer pheromone despite the presence of the pro-growth live *E. coli* is dependent on the organismal sensitivity to neuronal eIF2α phosphorylation mediated by eIF2Bα and eIF2γ, as the corresponding eIF2(αP)-insensitive mutations suppressed the pro-dauer effects (Figure 5C). These observations highlight the roles of the molecular determinants of eIF2α phosphorylation, EIF-2Ba and EIF-2c, in mediating the dauer developmental decision not only in the context of neuronal UPR activation (Figure 1A and Table 1), but also in the modulation of food-dependent sensitivity to ascarosides by constitutive neuronal eIF2α phosphorylation (Figure 5C). Collectively, our findings indicate that aberrant eIF2α status in the sensory neurons can confer dramatic responses that phenocopy starvation in adults, as well as modulating or synergistic effects on the dauer developmental decision.

Phosphorylation state of eIF2α in the ASI sensory neuron pair regulates organismal physiology

eIF2α phosphorylation is an evolutionarily conserved mechanism of nutrient detection in the unicellular yeast, as uncharged tRNAs symptomatic of amino acid deprivation activate the GCN2 eIF2α kinase. (Hinnebusch, 1994 and Wek et al., 1995). While cellular consequences of eIF2α phosphorylation have been extensively characterized in yeast (reviewed in Sonenberg and Hinnebusch, 2009), physiological systemic roles of the conserved translational control mechanism have been highlighted in recent studies, particularly in the nervous system.

Specifically, a broad array of complex biological processes in mammals including foraging, learning, addiction and imprinting have been shown to be modulated by eIF2α phosphorylation in the central nervous system (Hao et al., 2005, Costa-Mattioli et al., 2007, Stern et al., 2013, Huang et al., 2016 and Batista et al., 2016). We have demonstrated that constitutive phosphorylation of eIF2α in the ASI chemosensory neurons results in defects in growth rate, progeny production and fat storage (Figure 4). These systemic impairments are similar to those manifested when the animals are exposed to nutritionally limited conditions, reminiscent of the phenotypes exhibited by the *eat* mutants that are defective in food intake (Avery 1993, Lakowski and Hekimi, 1998 and Figure S4). That the organismal effects of neuronal eIF2(αP) on the adult worms mimic a starvation response is consistent with the triggering molecular event (eIF2α phosphorylation) and its site of action (ASI neurons). Our data therefore suggest that stress-induced eIF2α phosphorylation in the nervous system plays a critical role in inter-tissue communication and coordination, regulating diverse physiological outputs in *C. elegans*. Such systemic effects of eIF2α-mediated translational control illustrate how multicellular organisms may co-opt conserved stress signaling pathways that maintain cellular homeostasis to modulate organism-wide responses to environmental fluctuations and challenges.

Figure Legends

Figure 1: Identification of genes functioning in the ASI neurons to promote the dauer developmental decision in response to neuronal UPR activation and subsequent eIF2α phosphorylation

A. Schematic illustrating the alleles and gene products characterized in the study. Molecular identities of the alleles are listed in Table 1.

B. Fractions of the animals with indicated genotypes that form dauers at 25 °C. *eif-2Ba* was overexpressed specifically in the ASI neurons using the ASI-specific promoter *str-3p*. *eif-2Ba(qd335);daf-28(sa191)* presented were pooled from non-transgenic animals, all of which exhibited similar dauer entry frequencies. Plotted is mean ± SD. N represents total number of animals for each of the three independent transgenic lines.

Figure 2: The *eif-2c(qd336)* allele, encoding a mutant *C. elegans* ortholog of the gamma subunit of eIF2, alters sensitivity to eIF2α phosphorylation and translational requirements of eIF2B

A. Schematic illustrating the *qd336* variant of EIF-2c and its alteration of function in the context of translation initiation.

B. Fractions of the animals from wild-type versus *eif-2c(qd336)* backgrounds that reach reproductive maturation under RNAi conditions that downregulate indicated eIF2B subunits, representative of three independent experiments. Plotted is mean ± SD. N represents total number of animals for each condition. eIF2Bα is the only eIF2B subunit that is dispensable for viability.

C. Fractions of the animals from wild-type versus *eif-2c(qd336)* backgrounds that reach reproductive maturation under RNAi conditions that downregulate indicated eIF2 subunits. Plotted is mean ± SD. N represents total number of animals for each condition.

D. Fractions of the animals with indicated genotypes conferring eIF2(αP) insensitivity that reach reproductive maturation under RNAi conditions that downregulate eIF2Bγ. Plotted is mean ± SD. N represents total number of animals for each condition.

Figure 3: Constitutive eIF2α phosphorylation in ASI impairs growth, metabolism and reproduction, phenocopying the organismal responses to starvation

A. Bright-field imaging of age-matched adult animals from wild-type versus *qdIs10[gpa-4p::eIF2α(S49D)]* backgrounds.

B. Body length measurements, based on 10 representative, age-matched animals from wild-type versus *qdIs10[gpa-4p::eIF2α(S49D)]* backgrounds. Plotted is mean ± SD.

C. Body width measurements, based on 10 representative, age-matched animals from wild-type versus *qdIs10[gpa-4p::eIF2α(S49D)]* backgrounds. Plotted is mean ± SD

D. Growth rate of animals with indicated genotypes at 25 °C. Young adults refer to animals that have undergone the fourth larval molt. Notably, fertilized embryos start to become visible *in utero* in these animals.

E. Total number of progeny production in the animals from wild-type versus *qdIs10[gpa-4p::eIF2α(S49D)]* backgrounds, representative of three independent experiments. Plotted is mean ± SD.

F. Number of fertilized embryos observed in the hermaphrodite animals from wild-type versus *qdIs10[gpa-4p::eIF2α(S49D)]* backgrounds. Plotted is mean ± SD.

G. Egg-laying period of the animals from wild-type versus *qdIs10[gpa-4p::eIF2α(S49D)]* backgrounds, representative of three independent experiments. Plotted is mean ± SD.

H. Lipid staining of age-matched adult animals with indicated genotypes.

I. Fluorescence microscopy of the animals with indicated genotypes carrying the *hjIs67[atgl-1p::atgl-1::GFP]* transgene. The co-transformation marker of *qdIs10[gpa-4p::eIF2α(S49D)], ofm-1p::GFP,* also expresses GFP in the coelomocytes.

Figure 4: The effects of constitutive eIF2α phosphorylation in ASI on organismal physiology are distinct from those conferred by ASI ablation and are mediated by molecular determinants of sensitivity to eIF2α phosphorylation

A. Total number of progeny production of the *qdIs10[gpa-4p::eIF2α(S49D)]* animals carrying indicated mutations that confer eIF2(αP) insensitivity. Plotted is mean ± SD. Asterisks indicate statistical significance, $p < 0.01$, as determined by two-tailed Student's t-test (*qdIs10* versus *qdIs10* in the presence of eIF2(αP)-insensitive mutations).

B. Egg-laying period of the animals with indicated genotypes. Plotted is mean ± SD.

C. Total number of progeny production of the animals the ASI neurons of which have been genetically ablated. Plotted is mean ± SD. *csp-1b,* encoding a caspase ortholog, was expressed under the ASI-specific promoter *daf-7p* in the *qdEx47* transgene. Ablation of ASI was confirmed by dauer entry (Bargmann and Horvitz, 1991). Only animals that had entered dauer diapause and recovered were assayed for progeny production.

D. Egg-laying period of the animals with indicated genotypes. Plotted is mean ± SD.

Figure 5: Aberrant eIF2α phosphorylation in the ASI chemosensory neurons modulates the dauer developmental decision in response to neuroendocrine and environmental signals

A. Fractions of the indicated neuroendocrine pathway mutants, in the presence or absence of the *qdIs10[gpa-4p::eIF2α(S49D)]* transgene, that form dauer at 25 ºC. Plotted is mean ± SD. N represents total number of animals for each genotype. Results shown here are representative of three independent experiments.

B. Fractions of the animals from wild-type versus *qdIs10[gpa-4p::eIF2α(S49D)]* backgrounds that form dauer at 25 ºC, in the presence of ascarosides and indicated food sources. Plotted is mean ± SD. Results shown here are representative of three independent experiments.

C. Fractions of the animals from wild-type versus *qdIs10[gpa-4p::eIF2α(S49D)]* backgrounds that form dauer at 25 ºC, in the presence of ascarosides and live bacteria. Plotted is mean ± SD. Results shown here are representative of five independent experiments.

Author contributions

WK and DHK conceived research. WK performed experiments. HS assisted with experiments in Figures 2 and 3. YKZ and FCS provided ascarosides used in Figure 5. WK and DHK wrote the manuscript.

Acknowledgements

We thank the Caenorhabditis Genetics Center (CGC), which is supported by the NIH—National Center for Research Resources, and S. Mitani and the National BioResource Project (NBRP) for

providing strains used in this study. We thank Joshua Meisel and Zoë Hilbert for strains carrying the *qdEx47* transgene. This work was supported by NIH Grant GM084477 (to D.H.K.).

References

Angelo, G., and M. R. Van Gilst, 2009 Starvation protects germline stem cells and extends reproductive longevity in C. elegans. Science 326: 954-958.

Avery, L., 1993 The genetics of feeding in Caenorhabditis elegans. Genetics 133: 897-917.

Bargmann, C. I., and H. R. Horvitz, 1991 Control of larval development by chemosensory neurons in Caenorhabditis elegans. Science 251: 1243-1246.

Batista, G., J. L. Johnson, E. Dominguez, M. Costa-Mattioli and J. L. Pena, 2016 Translational control of auditory imprinting and structural plasticity by eIF2α. Elife 5.

Bishop, N. A., and L. Guarente, 2007 Two neurons mediate diet-restriction-induced longevity in C. elegans. Nature 447: 545-549.

Borck, G., B. S. Shin, B. Stiller, A. Mimouni-Bloch, H. Thiele et al., 2012 eIF2γ mutation that disrupts eIF2 complex integrity links intellectual disability to impaired translation initiation. Mol Cell 48: 641-646.

Brenner, S., 1974 The genetics of Caenorhabditis elegans. Genetics 77: 71-94.

Bugiani, M., I. Boor, J. M. Powers, G. C. Scheper and M. S. van der Knaap, 2010 Leukoencephalopathy with vanishing white matter: a review. J Neuropathol Exp Neurol 69: 987-996.

Cao, S. S., M. Wang, J. C. Harrington, B. M. Chuang, L. Eckmann et al., 2014 Phosphorylation of eIF2α is dispensable for differentiation but required at a posttranscriptional level for paneth cell function and intestinal homeostasis in mice. Inflamm Bowel Dis 20: 712-722.

Cassada, R. C., and R. L. Russell, 1975 The dauerlarva, a post-embryonic developmental variant of the nematode Caenorhabditis elegans. Dev Biol 46: 326-342.

Cornils, A., M. Gloeck, Z. Chen, Y. Zhang and J. Alcedo, 2011 Specific insulin-like peptides encode sensory information to regulate distinct developmental processes. Development 138: 1183-1193.

Costa-Mattioli, M., D. Gobert, E. Stern, K. Gamache, R. Colina et al., 2007 eIF2alpha phosphorylation bidirectionally regulates the switch from short- to long-term synaptic plasticity and memory. Cell 129: 195-206.

Di Prisco, G. V., W. Huang, S. A. Buffington, C. C. Hsu, P. E. Bonnen et al., 2014 Translational control of mGluR-dependent long-term depression and object-place learning by eIF2α. Nat Neurosci 17: 1073-1082.

Elsby, R., J. F. Heiber, P. Reid, S. R. Kimball, G. D. Pavitt et al., 2011 The alpha subunit of eukaryotic initiation factor 2B (eIF2B) is required for eIF2-mediated translational suppression of vesicular stomatitis virus. J Virol 85: 9716-9725.

Erickson, F. L., and E. M. Hannig, 1996 Ligand interactions with eukaryotic translation initiation factor 2: role of the gamma-subunit. EMBO J 15: 6311-6320.

Erickson, F. L., J. Nika, S. Rippel and E. M. Hannig, 2001 Minimum requirements for the function of eukaryotic translation initiation factor 2. Genetics 158: 123-132.

Evans, T. C., 2006 Transformation and Injection. WormBook: 1-15.

Fielenbach, N., and A. Antebi, 2008 C. elegans dauer formation and the molecular basis of plasticity. Genes Dev 22: 2149-2165.

Freyaldenhoven, S., Y. Li, A. M. Kocabas, E. Ziu, S. Ucer et al., 2012 The role of ERp44 in maturation of serotonin transporter protein. J Biol Chem 287: 17801-17811.

Hannig, E. M., and A. G. Hinnebusch, 1988 Molecular analysis of GCN3, a translational activator of GCN4: evidence for posttranslational control of GCN3 regulatory function. Mol Cell Biol 8: 4808-4820.

Hao, S., J. W. Sharp, C. M. Ross-Inta, B. J. McDaniel, T. G. Anthony et al., 2005 Uncharged tRNA and sensing of amino acid deficiency in mammalian piriform cortex. Science 307: 1776-1778.

Higo, T., M. Hattori, T. Nakamura, T. Natsume, T. Michikawa et al., 2005 Subtype-specific and ER lumenal environment-dependent regulation of inositol 1,4,5-trisphosphate receptor type 1 by ERp44. Cell 120: 85-98.

Hinnebusch, A. G., 1997 Translational regulation of yeast GCN4. A window on factors that control initiator-trna binding to the ribosome. J Biol Chem 272: 21661-21664.

Hinnebusch, A. G., 2005 Translational regulation of GCN4 and the general amino acid control of yeast. Annu Rev Microbiol 59: 407-450.

Hisatsune, C., E. Ebisui, M. Usui, N. Ogawa, A. Suzuki et al., 2015 ERp44 Exerts Redox-Dependent Control of Blood Pressure at the ER. Mol Cell 58: 1015-1027.

Hu, P. J., 2007 Dauer. WormBook: 1-19.

Huang, W., A. N. Placzek, G. Viana Di Prisco, S. Khatiwada, C. Sidrauski *et al.*, 2016 Translational control by eIF2α phosphorylation regulates vulnerability to the synaptic and behavioral effects of cocaine. Elife 5.

Hung, W. L., Y. Wang, J. Chitturi and M. Zhen, 2014 A Caenorhabditis elegans developmental decision requires insulin signaling-mediated neuron-intestine communication. Development 141: 1767-1779.

Jansen, G., K. L. Thijssen, P. Werner, M. van der Horst, E. Hazendonk et al., 1999 The complete family of genes encoding G proteins of Caenorhabditis elegans. Nat Genet 21: 414-419.

Jennings, M. D., C. J. Kershaw, C. White, D. Hoyle, J. P. Richardson et al., 2016 eIF2β is critical for eIF5-mediated GDP-dissociation inhibitor activity and translational control. Nucleic Acids Res.

Jennings, M. D., and G. D. Pavitt, 2010 eIF5 has GDI activity necessary for translational control by eIF2 phosphorylation. Nature 465: 378-381.

Jeong, P. Y., M. Jung, Y. H. Yim, H. Kim, M. Park et al., 2005 Chemical structure and biological activity of the Caenorhabditis elegans dauer-inducing pheromone. Nature 433: 541-545.

Kashiwagi, K., M. Takahashi, M. Nishimoto, T. B. Hiyama, T. Higo et al., 2016 Crystal structure of eukaryotic translation initiation factor 2B. Nature 531: 122-125.

Kim, K., K. Sato, M. Shibuya, D. M. Zeiger, R. A. Butcher et al., 2009 Two chemoreceptors mediate developmental effects of dauer pheromone in C. elegans. Science 326: 994-998.

Kimura, K. D., H. A. Tissenbaum, Y. Liu and G. Ruvkun, 1997 daf-2, an insulin receptor-like gene that regulates longevity and diapause in Caenorhabditis elegans. Science 277: 942-946.

Kuhle, B., N. K. Eulig and R. Ficner, 2015 Architecture of the eIF2B regulatory subcomplex and its implications for the regulation of guanine nucleotide exchange on eIF2. Nucleic Acids Res 43: 9994-10014.

Kulalert, W., and D. H. Kim, 2013 The unfolded protein response in a pair of sensory neurons promotes entry of C. elegans into dauer diapause. Curr Biol 23: 2540-2545.

Lakowski, B., and S. Hekimi, 1998 The genetics of caloric restriction in Caenorhabditis elegans. Proc Natl Acad Sci U S A 95: 13091-13096.

Li, W., S. G. Kennedy and G. Ruvkun, 2003 daf-28 encodes a C. elegans insulin superfamily member that is regulated by environmental cues and acts in the DAF-2 signaling pathway. Genes Dev 17: 844-858.

Lin, Y., X. Pang, G. Huang, S. Jamison, J. Fang et al., 2014 Impaired eukaryotic translation initiation factor 2B activity specifically in oligodendrocytes reproduces the pathology of vanishing white matter disease in mice. J Neurosci 34: 12182-12191.

Malone, E. A., and J. H. Thomas, 1994 A screen for nonconditional dauer-constitutive mutations in Caenorhabditis elegans. Genetics 136: 879-886.

Maurin, A. C., C. Jousse, J. Averous, L. Parry, A. Bruhat *et al.*, 2005 The GCN2 kinase biases feeding behavior to maintain amino acid homeostasis in omnivores. Cell Metab 1**:** 273-277.

McGrath, P. T., Y. Xu, M. Ailion, J. L. Garrison, R. A. Butcher et al., 2011 Parallel evolution of domesticated Caenorhabditis species targets pheromone receptor genes. Nature 477: 321-325.

Park, D., I. O'Doherty, R. K. Somvanshi, A. Bethke, F. C. Schroeder et al., 2012 Interaction of structure-specific and promiscuous G-protein-coupled receptors mediates small-molecule signaling in Caenorhabditis elegans. Proc Natl Acad Sci U S A 109: 9917-9922.

Pavitt, G. D., K. V. Ramaiah, S. R. Kimball and A. G. Hinnebusch, 1998 eIF2 independently binds two distinct eIF2B subcomplexes that catalyze and regulate guanine-nucleotide exchange. Genes Dev 12: 514-526.

Pavitt, G. D., W. Yang and A. G. Hinnebusch, 1997 Homologous segments in three subunits of the guanine nucleotide exchange factor eIF2B mediate translational regulation by phosphorylation of eIF2. Mol Cell Biol 17: 1298-1313.

Pottekat, A., S. Becker, K. R. Spencer, J. R. Yates, G. Manning et al., 2013 Insulin biosynthetic interaction network component, TMEM24, facilitates insulin reserve pool release. Cell Rep 4: 921-930.

Pungaliya, C., J. Srinivasan, B. W. Fox, R. U. Malik, A. H. Ludewig *et al.*, 2009 A shortcut to identifying small molecule signals that regulate behavior and development in Caenorhabditis elegans. Proc Natl Acad Sci U S A 106**:** 7708-7713.

Ravindran, R., J. Loebbermann, H. I. Nakaya, N. Khan, H. Ma et al., 2016 The amino acid sensor GCN2 controls gut inflammation by inhibiting inflammasome activation. Nature 531: 523-527.

Roll-Mecak, A., P. Alone, C. Cao, T. E. Dever and S. K. Burley, 2004 X-ray structure of translation initiation factor eIF2gamma: implications for tRNA and eIF2alpha binding. J Biol Chem 279: 10634-10642.

Sekine, Y., A. Zyryanova, A. Crespillo-Casado, P. M. Fischer, H. P. Harding et al., 2015 Stress responses. Mutations in a translation initiation factor identify the target of a memory-enhancing compound. Science 348: 1027-1030.

Sidrauski, C., J. C. Tsai, M. Kampmann, B. R. Hearn, P. Vedantham et al., 2015 Pharmacological dimerization and activation of the exchange factor eIF2B antagonizes the integrated stress response. Elife 4: e07314.

Sonenberg, N., and A. G. Hinnebusch, 2009 Regulation of translation initiation in eukaryotes: mechanisms and biological targets. Cell 136: 731-745.

Stern, E., A. Chinnakkaruppan, O. David, N. Sonenberg and K. Rosenblum, 2013 Blocking the eIF2α kinase (PKR) enhances positive and negative forms of cortex-dependent taste memory. J Neurosci 33**:** 2517-2525.

Vazquez de Aldana, C. R., T. E. Dever and A. G. Hinnebusch, 1993 Mutations in the alpha subunit of eukaryotic translation initiation factor 2 (eIF-2 alpha) that overcome the inhibitory effect of eIF-2 alpha phosphorylation on translation initiation. Proc Natl Acad Sci U S A 90: 7215-7219.

Wang, J., T. Takeuchi, S. Tanaka, S. K. Kubo, T. Kayo et al., 1999 A mutation in the insulin 2 gene induces diabetes with severe pancreatic beta-cell dysfunction in the Mody mouse. J Clin Invest 103: 27-37.

Wek, R. C., H. Y. Jiang and T. G. Anthony, 2006 Coping with stress: eIF2 kinases and translational control. Biochem Soc Trans 34: 7-11.

Williams, D. D., G. D. Pavitt and C. G. Proud, 2001 Characterization of the initiation factor eIF2B and its regulation in Drosophila melanogaster. J Biol Chem 276: 3733-3742.

Yang, K., D. F. Li, X. Wang, J. Liang, R. Sitia et al., 2016 Crystal Structure of the ERp44-Peroxiredoxin 4 Complex Reveals the Molecular Mechanisms of Thiol-Mediated Protein Retention. Structure.

Yang, W., and A. G. Hinnebusch, 1996 Identification of a regulatory subcomplex in the guanine nucleotide exchange factor eIF2B that mediates inhibition by phosphorylated eIF2. Mol Cell Biol 16: 6603-6616.

Figure 1

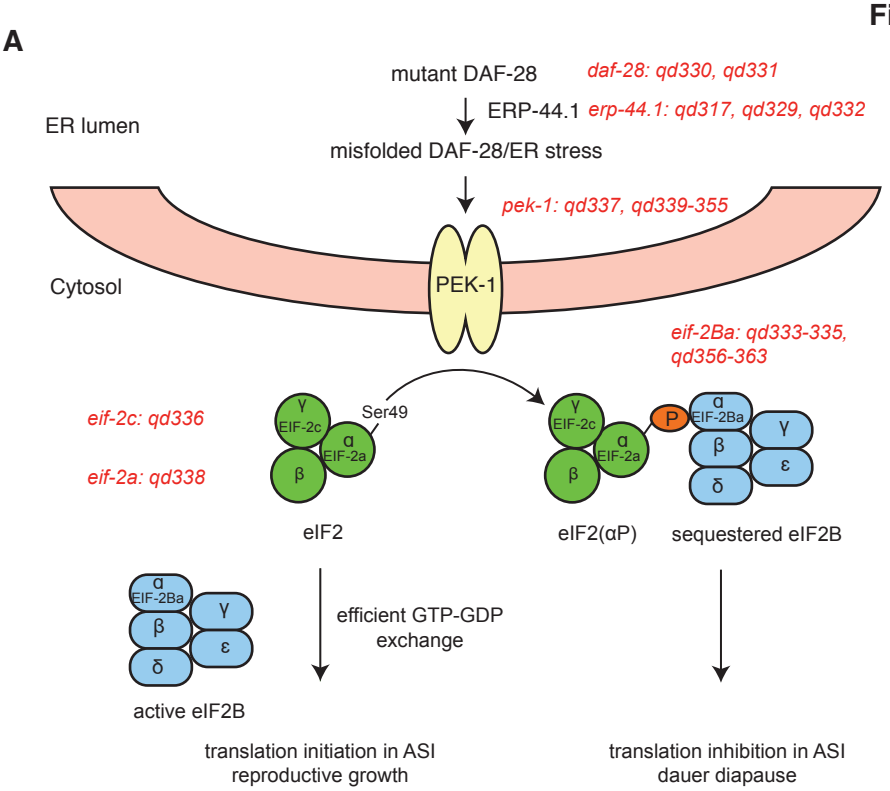
A
mutant DAF-28
daf-28: qd330, qd331
ERP-44.1
erp-44.1: qd317, qd329, qd332
ER lumen
misfolded DAF-28/ER stress
pek-1: qd337, qd339-355
Cytosol
PEK-1
eif-2Ba: qd333-335, qd356-363
eif-2c: qd336
eif-2a: qd338
Ser49
γ EIF-2c
α EIF-2a
β
P
α EIF-2Ba
γ
β
δ
ε
eIF2
eIF2(αP)
sequestered eIF2B
active eIF2B
efficient GTP-GDP exchange
translation initiation in ASI reproductive growth
translation inhibition in ASI dauer diapause

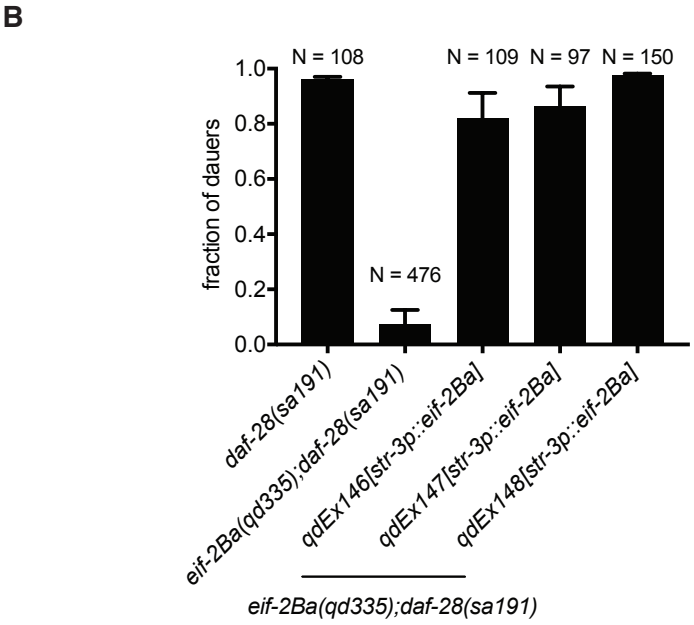
B
N = 108
N = 109
N = 97
N = 150
N = 476
fraction of dauers
1.0
0.8
0.6
0.4
0.2
0.0
daf-28(sa191)
eif-2Ba(qd335);daf-28(sa191)
qdEx146[str-3p::eif-2Ba]
qdEx147[str-3p::eif-2Ba]
qdEx148[str-3p::eif-2Ba]
eif-2Ba(qd335);daf-28(sa191)

Figure 2

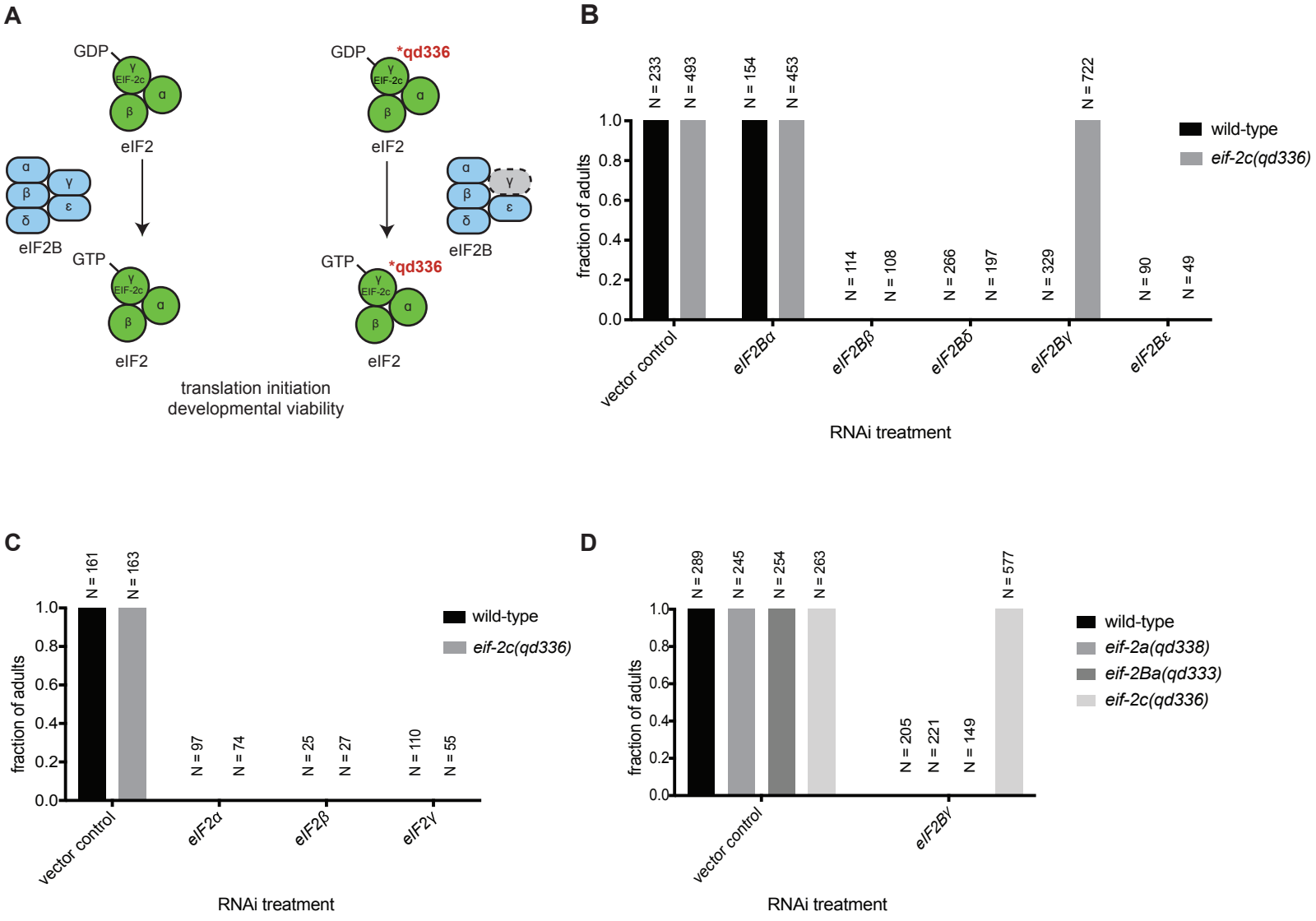
A
GDP
eIF2
eIF2B
GTP
*qd336
translation initiation
developmental viability
B
fraction of adults
RNAi treatment
vector control
eIF2Bα
eIF2Bβ
eIF2Bδ
eIF2Bγ
eIF2Bε
wild-type
eif-2c(qd336)
C
eIF2α
eIF2β
eIF2γ
D
eif-2a(qd338)
eif-2Ba(qd333)

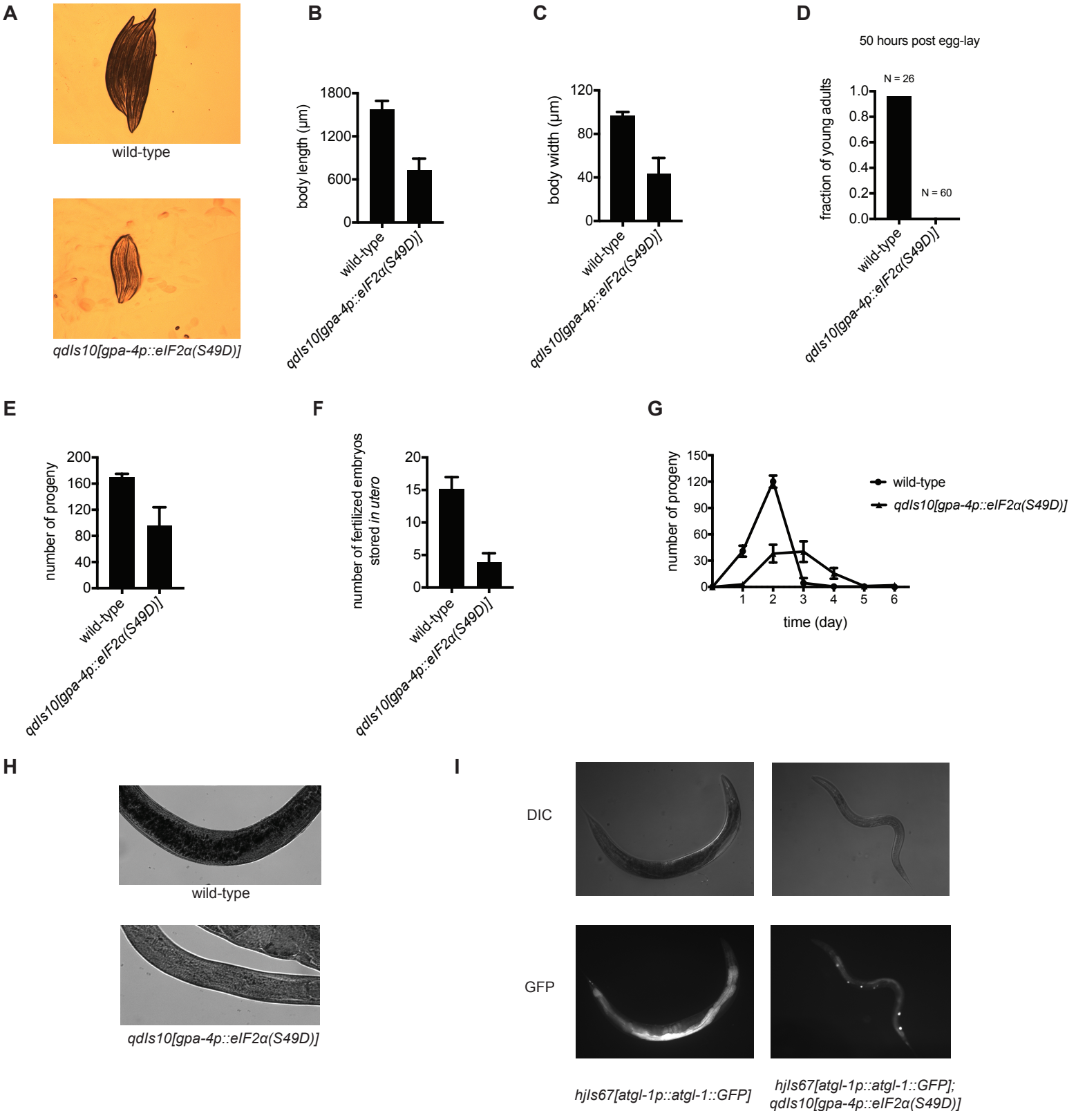
A
wild-type
qdIs10[gpa-4p::eIF2α(S49D)]
B
body length (µm)
1800
1200
600
0
wild-type
qdIs10[gpa-4p::eIF2α(S49D)]
C
body width (µm)
120
80
40
0
wild-type
qdIs10[gpa-4p::eIF2α(S49D)]
D
50 hours post egg-lay
fraction of young adults
1.0
0.8
0.6
0.4
0.2
0.0
N = 26
N = 60
wild-type
qdIs10[gpa-4p::eIF2α(S49D)]
E
number of progeny
200
160
120
80
40
0
wild-type
qdIs10[gpa-4p::eIF2α(S49D)]
F
number of fertilized embryos stored in utero
20
15
10
5
0
wild-type
qdIs10[gpa-4p::eIF2α(S49D)]
G
number of progeny
150
120
90
60
30
0
1
2
3
4
5
6
time (day)
wild-type
qdIs10[gpa-4p::eIF2α(S49D)]
H
wild-type
qdIs10[gpa-4p::eIF2α(S49D)]
I
DIC
GFP
hjIs67[atgl-1p::atgl-1::GFP]
hjIs67[atgl-1p::atgl-1::GFP];
qdIs10[gpa-4p::eIF2α(S49D)]

Figure 4

A

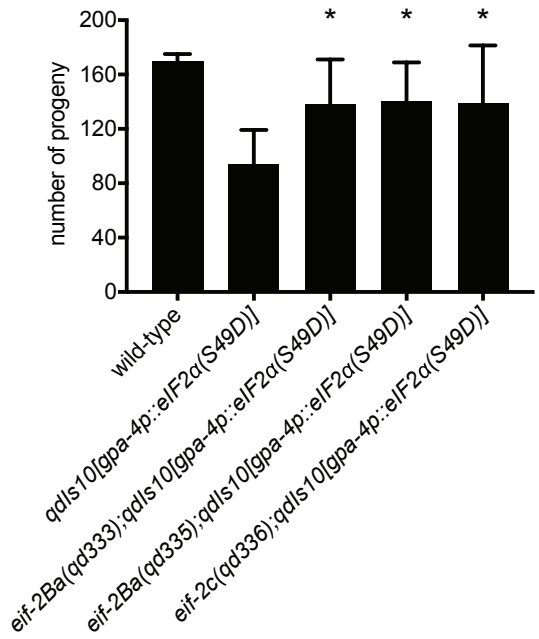

B

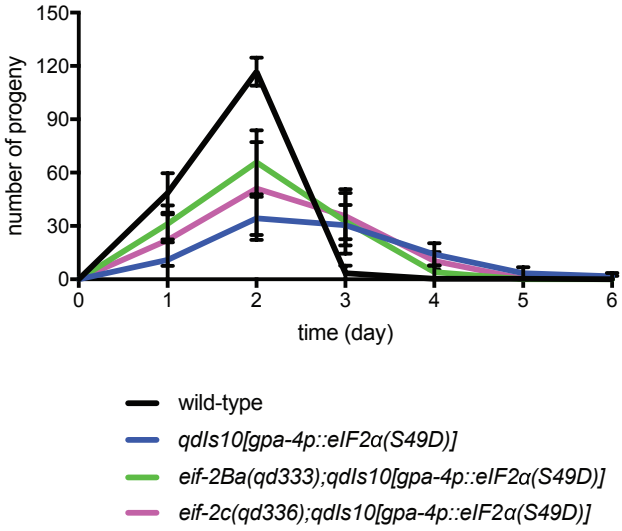

C

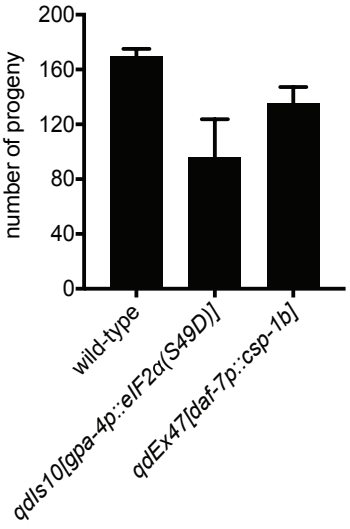

D

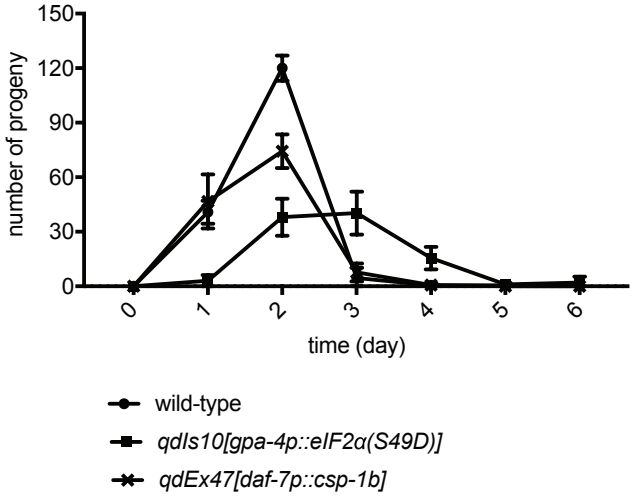

Figure 5

A

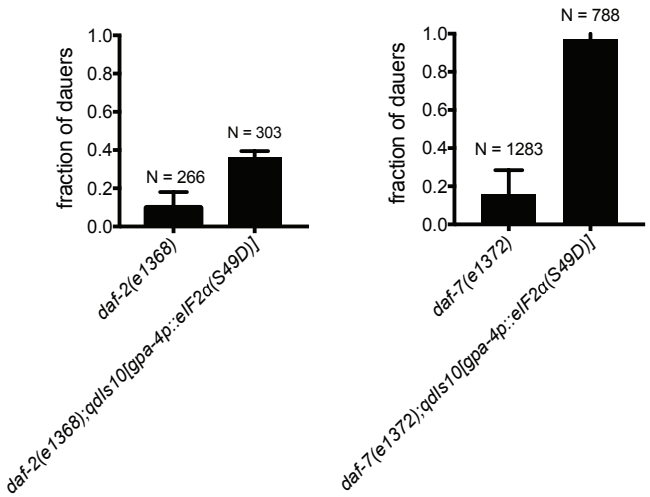
fraction of dauers
1.0
0.8
0.6
0.4
0.2
0.0
N = 266
N = 303
daf-2(e1368)
daf-2(e1368);qdIs10[gpa-4p::eIF2α(S49D)]
N = 1283
N = 788
daf-7(e1372)
daf-7(e1372);qdIs10[gpa-4p::eIF2α(S49D)]

B

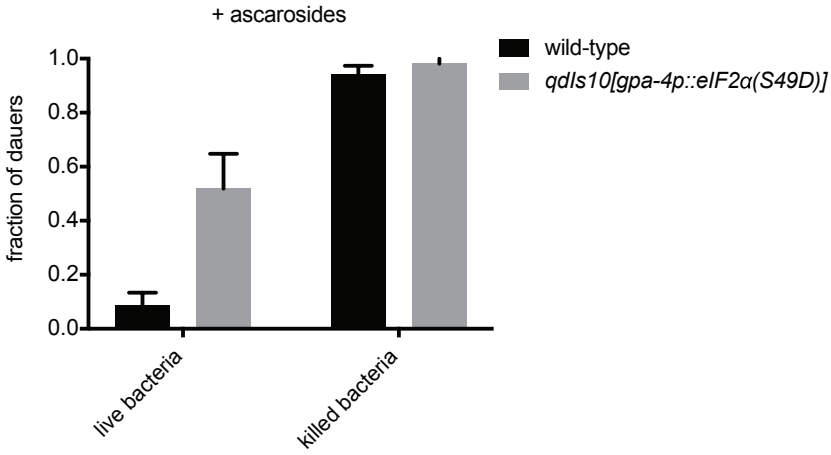
+ ascarosides
wild-type
qdIs10[gpa-4p::eIF2α(S49D)]
fraction of dauers
1.0
0.8
0.6
0.4
0.2
0.0
live bacteria
killed bacteria

C

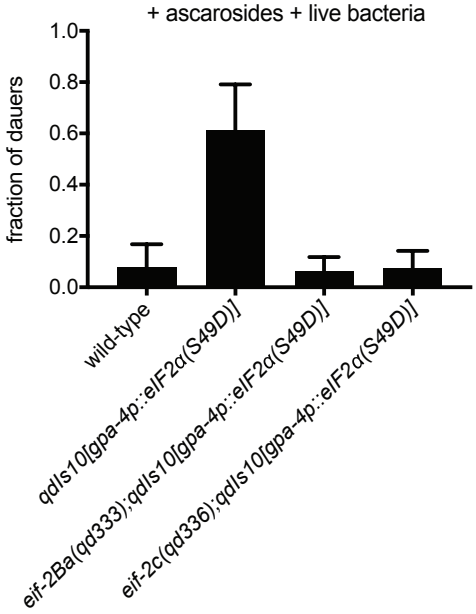
+ ascarosides + live bacteria
fraction of dauers
1.0
0.8
0.6
0.4
0.2
0.0
wild-type
qdIs10[gpa-4p::eIF2α(S49D)]
eif-2Ba(qd333);qdIs10[gpa-4p::eIF2α(S49D)]
eif-2c(qd336);qdIs10[gpa-4p::eIF2α(S49D)]